

Nonclassicality of photons in mean-field anisotropic quantum light-matter interacting lattices: Two-photon correlation function and quadrature squeezing

Xu-Min Chen(陈许敏), Pei-Yao Chen(陈佩瑶), and Chen Wang(王晨)

Citation: Chin. Phys. B, 2025, 34 (**4**): 044201. DOI: 10.1088/1674-1056/ada9db
Journal homepage: http://cpb.iphy.ac.cn; http://iopscience.iop.org/cpb

What follows is a list of articles you may be interested in

Four-wave mixing Bragg scattering for small frequency shift from silicon coupled microrings

Chang Zhao(赵畅), Chao Wu(吴超), Pingyu Zhu(朱枰谕), Yuxing Du(杜昱星), Yan Wang(王焱), Miaomiao Yu(余苗苗), Kaikai Zhang(张凯凯), and Ping Xu(徐平)
Chin. Phys. B, 2025, 34 (**1**): 014206. DOI: 10.1088/1674-1056/ad8a4f

Enhanced sensing of anharmonicities in a gain-based anti-PT symmetric system

Ya-Wei Zeng(曾亚伟), Tian-Le Yang(杨天乐), Qi-Yin Lin(林琪茵), and Wan-Jun Su(苏万钧)
Chin. Phys. B, 2024, 33 (**12**): 124201. DOI: 10.1088/1674-1056/ad8a4d

Superradiance of ultracold cesium Rydberg $|65D_{5/2}> \rightarrow |66P_{3/2}>$

Liping Hao(郝丽萍), Xiaoxuan Han(韩小萱), Suying Bai(白素英), Xiufen You(游秀芬), Yuechun Jiao(焦月春), and Jianming Zhao(赵建明)
Chin. Phys. B, 2024, 33 (**5**): 054204. DOI: 10.1088/1674-1056/ad20da

Versatile and controlled quantum teleportation network

Yao-Yao Zhou(周瑶瑶), Peng-Xian Mei(梅鹏娴), Yan-Hong Liu(刘艳红), Liang Wu(吴量), Yan-Xiang Li(李雁翔), Zhi-Hui Yan(闫智辉), and Xiao-Jun Jia(贾晓军)
Chin. Phys. B, 2024, 33 (**3**): 034209. DOI: 10.1088/1674-1056/ad1981

Gigahertz frequency hopping in an optical phase-locked loop for Raman lasers

Dekai Mao(毛德凯), Hongmian Shui(税鸿冕), Guoling Yin(殷国玲), Peng Peng(彭鹏), Chunwei Wang(王春唯), and Xiaoji Zhou(周小计)
Chin. Phys. B, 2024, 33 (**2**): 024209. DOI: 10.1088/1674-1056/ad174b

---

Nonclassicality of photons in mean-field anisotropic quantum light–matter interacting lattices: Two-photon correlation function and quadrature squeezing

Xu-Min Chen(陈许敏)[1], Pei-Yao Chen(陈佩瑶)[1], and Chen Wang(王晨)[2,†]

[1] *Department of Physics, Hangzhou Dianzi University, Hangzhou* 310018, *China*
[2] *Department of Physics, Zhejiang Normal University, Jinhua* 321004, *China*

(Received 10 November 2024; revised manuscript received 28 December 2024; accepted manuscript online 14 January 2025)

The generation of nonclassical photons via quantum light–matter interactions is of fundamental importance in quantum optics. Here we investigate steady-state two-photon correlation function and photon squeezing in an open anisotropic Rabi lattice by applying quantum dressed master equation embedded with the mean-field approximation. The expanded antibunching effect of photons due to anisotropic qubit–photon interaction, is strongly suppressed by including inter-site photon tunneling, whereas the giant photon bunching keeps robust with weak inter-site photon tunneling strength. The microscopic processes for photon antibunching and bunching effects are presented based on incoherent transitions between eigenstates. The photon squeezing is also analyzed under the influences of qubit–photon coupling and anisotropic factor. The quadrature squeezing shows persistency by tuning on the inter-site photon tunneling, and becomes dramatically pronounced at the small anisotropic factor. Moreover, the increasing number of qubits significantly enhances quadrature squeezing with strong qubit–photon interaction. We hope such results may provide physical insights into efficient generation and manipulation of nonclassical features of photons in quantum light–matter interacting lattice systems.

Keywords: quantum optics, photon statistics and coherence theory, coherent control of atomic interactions with photons

PACS: 42.50.–p, 42.50.Ar, 32.80.Qk

DOI: 10.1088/1674-1056/ada9db **CSTR:** 32038.14.CPB.ada9db

1. Introduction

The microscopic description of quantum interaction between the radiation field and matter structure plays a crucial role in understanding the quantum electrodynamics (QED),[1] which spurs the advancements of quantum optics,[2] quantum information processing,[3] and quantum thermodynamics.[4,5] The natural atoms embedded in optical cavity are generally weakly coupled to photons, nowadays called cavity-QED.[6] While the solid-state qubits interacting with microwave resonators construct the circuit-QED (cQED).[7] cQED is able to achieve strong, ultrastrong, and even deepstrong qubit–photon couplings by surmounting the dipole light–matter interaction limit.[8–11]

Recently, the anisotropic effect of quantum light–matter interacting systems has attracted increasing attention, representatively termed as anisotropic quantum Rabi model (aQRM),[12–14] where the coupling strength of rotating-wave-terms is distinct from the counter-rotating terms. aQRM has been experimentally realized in various setups, e.g., one qubit interacting with single-mode bosonic field describing cross-electric and magnetic fields[12,15] and semiconductor electrons with Rashba and Dressulhaus spin–orbital couplings.[16,17]

When considering the photon tunneling between neighbouring cavities, cQED setups can be extended to the cQED dimer,[18,19] ring,[20,21] lattice,[22–26] and quantum network[27–30] structures, boosting the development of quantum phase transition of light both at ground state and steady state with quantum dissipation.[31,32] Theoretically, cQED lattices systems can be modelled as the generic Rabi–Hubbard lattice[33,34] and Jaynes–Cummings–Hubbard lattice[22,23] with strong and weak qubit–photon couplings, respectively. In particular, by tuning on inter-site photon tunneling the localization–delocalization of photons can be intriguingly exhibited both with analytical and numerical approaches.[31] If multiple qubits are embedded in each cavity, the hybrid chain system is described as the Dicke–Hubbard model,[31,35] which fertilizes the phase diagram of photons.

Recently, various emerging phenomena, e.g., many body localization,[36] bound states,[37–39] and topological pumping,[40,41] have been observed in light–material interacting lattices, which is unavailable in the single-site hybrid systems. Considering the importance of generating nonclassical photon resources from photonic lattices,[42–45] it should be intriguing to explore the correlation and nonclassicality of photons in quantum light–matter interacting lattices.

The generation of nonclassical photons is a long-standing

†Corresponding author. E-mail: wangchen@zjnu.cn

© 2025 Chinese Physical Society and IOP Publishing Ltd. All rights, including for text and data mining, AI training, and similar technologies, are reserved.

topic in quantum light–matter interacting systems, e.g., open optomechanical system[46] and quantum Rabi model.[48] Two main features are the two-photon statistics[49,50] and photon squeezing.[51–53] Specifically, two-photon statistics quantify the quantumness of photons, e.g., antibunching effect. Glauber initially proposed such pioneering concept to trigger the advent of quantum optics.[54] As the qubit–photon interaction becomes strong, the quantum light–matter interacting systems should be treated as a whole,[55,56] which naturally resulting in the dressed redefinition of two-photon correlations, as individually carried out by Rabl and Ridolfo *et al.* based on optomechanics[46,47] and cQEDs.[48,57] While photon squeezing characterizes reduction of the fluctuation of photon field below the Heisenberg noise limit.[58,59] The amplitude and phase of photon fields inevitably fluctuate under the law of quantum mechanics.[53] In particular for quadrature squeezing of photons, the noise of one quadrature component breaks the zero-point level, whereas the other component expectedly surpasses the vacuum state value.[60] Quadrature squeezing has been extensively applied to explore nonclassicality of photons in various quantum light–matter interacting systems.[61–66]

In this study, we combine the anisotropic qubit–photon interaction and inter-site photon tunneling to analyze their contributions to nonclassicality of photons, i.e., photon blockade and quadrature squeezing. In absence of inter-site photon tunneling, the antibunching regime of photons are dramatically expanded, compared to the standard QRM.[57] The antibunching effect of photons are strongly suppressed by inter-site photon tunneling, whereas the bunching feature is robust with weak inter-site photon tunneling strength. Moreover, the microscopic processes are established by incoherent transitions with lowest excited eigenstates constraint by parity selection coefficients. We also study photon squeezing by tuning qubit–photon coupling and anisotropic factor, where the quadrature squeezing becomes robust both with and without inter-site photon tunnelings. The global minimum of quadrature squeezing by tuning qubit–photon coupling favors inter-site photon tunneling at weak anisotropic factor regime. Furthermore, it is found that multiple qubits is helpful for enhancing squeezing effect with strong qubit–photon interaction.

The rest of this paper is organized as follows: In Section 2, we introduce the anisotropic Rabi lattice model. By including mean-field approximation, the Rabi lattice is simplified to the effective aQRM. Then we derive the quantum dressed master equation (DME)[55,56] to obtain the steady state. In Section 3, we analyze the effects of anisotropic qubit–photon interaction and inter-site photon tunneling on two-photon correlation function and quadrature squeezing. Finally we give a conclusion in Section 4.

2. Model and method

We first introduce the full Hamiltonian of the dissipative anisotropic Rabi lattice model.[31] Then we include the quantum master equation to obtain the dissipative dynamical equation of the effective single-site anisotropic Rabi model, where the mean-field theory is embedded to approximately treat the anisotropic Rabi lattice to the effective anisotropic Rabi model.

2.1. Anisotropic Rabi lattice

The dissipative anisotropic Rabi lattice, including three components, i.e., the anisotropic Rabi lattice, bosonic thermal reservoirs, and system–reservoir interactions, is described as

$$\hat{H}_{\rm tot} = \hat{H}_{\rm s} + \hat{H}_{\rm b} + \hat{V}. \tag{1}$$

$\hat{H}_{\rm s}$ denotes the anisotropic Rabi lattice Hamiltonian, which consists of on-site anisotropic quantum Rabi model (aQRM) and nearest-neighbouring inter-site photon tunneling in Fig. 1(a). It reads ($\hbar = 1$)

$$\hat{H}_{\rm s} = \sum_n \hat{H}_n^{\rm aRabi} - t \sum_{\langle n,m\rangle} (\hat{a}_n^\dagger \hat{a}_m + \hat{a}_m^\dagger \hat{a}_n). \tag{2}$$

$\hat{H}_n^{\rm aRabi}$ means the aQRM on the n-th site, including the anisotropic qubit–photon interactions, and the corresponding Hamiltonian is described as

$$\begin{aligned}\hat{H}_n^{\rm aRabi} =\ & \frac{\varepsilon}{2}\hat{\sigma}_z^n + \omega_0 \hat{a}_n^\dagger \hat{a}_n + \lambda[(\hat{a}_n^\dagger \hat{\sigma}_-^n + \hat{a}_n \hat{\sigma}_+^n) \\ & + \gamma(\hat{a}_n^\dagger \hat{\sigma}_+^n + \hat{a}_n \hat{\sigma}_-^n)],\end{aligned} \tag{3}$$

where $\hat{a}_n^\dagger$ ($\hat{a}_n$) creates (annihilates) one photon at the n-th site with the frequency ω_0, $\hat{\sigma}_\alpha^n$ ($\alpha = x, z, \pm$) show the Pauli operators, which is composed of two levels, i.e.,

$$\begin{aligned}&\hat{\sigma}_z^n = |\uparrow\rangle\langle\uparrow| - |\downarrow\rangle\langle\downarrow|, \quad \hat{\sigma}_+^n = |\uparrow\rangle\langle\downarrow|, \\ &\hat{\sigma}_-^n = (\hat{\sigma}_+^n)^\dagger, \quad \hat{\sigma}_x^n = \hat{\sigma}_+^n + \hat{\sigma}_-^n,\end{aligned}$$

and λ describes the qubit–photon coupling strength, γ denotes the anisotropic factor modulating the counter-rotating terms (CRTs), t is the inter-site photon tunneling strength, and $\langle n,m\rangle$ means that n and m are the nearest-neighbouring sites. In absence of γ, the aQRM is reduced to the seminal Jaynes–Cummings model, whereas the aQRM becomes the standard QRM as $\gamma = 1$. $\hat{H}_{\rm b} = \sum_{k;\nu=q,c} \omega_{k,\nu} \hat{b}_{k,\nu}^\dagger \hat{b}_{k,\nu}$, where $\hat{b}_{k,\nu}^\dagger$ ($\hat{b}_{k,\nu}$) creates (annihilates) one phonon in the ν-th reservoir having the frequency $\omega_{k,\nu}$ and mode k, and the linear system–reservoirs interactions are specified as

$$\hat{V}_q = \sum_{n,k} \hat{\sigma}_x^n (g_{n,k,q} \hat{b}_{k,q}^\dagger + g_{n,k,q}^* \hat{b}_{k,q}), \tag{4a}$$

$$\hat{V}_c = \sum_{n,k} (\hat{a}_n^\dagger + \hat{a}_n)(g_{n,k,c} \hat{b}_{k,c}^\dagger + g_{n,k,c}^* \hat{b}_{k,c}), \tag{4b}$$

with $g_{n,k,q}$ the coupling strength between the qubit on the n-th site and the q-th reservoir with the mode k, and $g_{n,k,c}$ the coupling strength between the resonator on the n-th site and the c-th reservoir with the mode k.

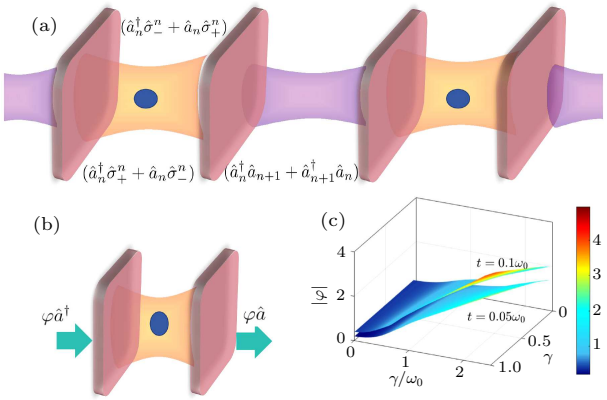


Fig. 1. (a) A schematic illustration of quantum light–matter interacting lattice at Eq. (2), which is composed of on-site anisotropic Rabi model in Eq. (3) and inter-site linear photon tunneling, (b) the effective mean-field anisotropic Rabi model in Eq. (7) with the order parameter of photons $\varphi=\langle\hat{a}\rangle$, in which the inter-site photon tunneling is effectively changed to the approximate external driving onto the on-site photons, and (c) the behavior of $|\varphi|$ by tuning the qubit–photon coupling strength λ and the anisotropic factor γ with distinct tunneling strengths t. Other system parameters are given by the photon frequency $\omega_0=1$, the qubit splitting energy $\varepsilon=\omega_0$, the nearest-neighbouring number $z=4$, the dissipation strengthes $\alpha_q=\alpha_c=10^{-4}$, the cut-off frequency of thermal reservoirs $\omega_c=20\omega_0$, and the temperatures of thermal reservoirs $k_BT_c=k_BT_q=0.1\omega_0$. These parameters are consistent with previous works,[9,11] e.g., $\omega_0/2\pi=6$ GHz, qubit $\varepsilon/2\pi=6$ GHz, λ able to reach even 7 GHz, $\alpha_q=2\times10^{-4}$, and $\alpha_c=2\times10^{-4}$. γ can be tuned from 0 to 1 by modulating the inductance of the circuit and the mutual inductance.[12,15] We select the two-dimensional square cQED lattice with $z=4$ as the generic case.[67] The temperatures of thermal reservoirs can be easily tuned up to 100 mK.[5]

Moreover, if we consider multiple qubits interacting with single-mode radiation field on-site, the aQRM is extended by the anisotropic Dicke model[68,69]

$$\hat{H}_n^{\text{aDicke}}=\varepsilon\hat{J}_z^n+\omega_0\hat{a}_n^\dagger\hat{a}_n+\frac{\lambda}{\sqrt{N_s}}[(\hat{a}_n^\dagger\hat{J}_-^n+\hat{a}_n\hat{J}_+^n)+\gamma(\hat{a}_n^\dagger\hat{J}_+^n+\hat{a}_n\hat{J}_-^n)], \tag{5}$$

where $\hat{J}_\alpha^n=\sum_{i=1}^{N_s}\hat{\sigma}_{\alpha,i}^n$ $(\alpha=x,z,\pm)$ shows the collective angular momentum operator, which is composed of N_s two levels, i.e., $\hat{\sigma}_z=|\uparrow\rangle\langle\uparrow|-|\downarrow\rangle\langle\downarrow|$, $\hat{\sigma}_+^n=|\uparrow\rangle\langle\downarrow|$, $\hat{\sigma}_-=(\hat{\sigma}_+^n)^\dagger$, and $\hat{\sigma}_x=\hat{\sigma}_++\hat{\sigma}_-$, and N_s is the qubits number.

The quantum phase transition of light in quantum light–matter interacting systems has been extensively proposed and analyzed.[22–24] In the past decade, there exist several experimental advance in realizing circuit-QED large arrays.[31,70] In particular, the nearest-neighbouring coupling of cavities can be conducted via a capacitive or Josephson coupling.[71] Moreover, we consider the inter-site coupling strength is much smaller than the frequency of the on-site cavity, which leads to the inter-site photon tunneling. While for the on-site anisotropic qubit–photon interactions, it may be realized based on the superconducting circuits.[12,15] One main superconducting quantum interference device (SQUID) with a larger circuit triggers an electromagnetic field, which is inductively coupled to the other SQUID loop. By ignoring capacitive interaction between such two SQUIDs, the anisotropic qubit–photon coupling can be steadily generated by including both inductance of circuits and the mutual inductance. And quantum thermal reservoirs can be mimicked by long transmission lines, which correspond to a huge number of modes of harmonic oscillators.

2.2. Quantum master equation

Practically, quantum systems inevitably interact with the environment via the dissipative energy exchange processes as also shown in Eqs. (4a) and (4b). We assume the system–reservoir interactions on each site are weak, which may be properly perturbed to generate the dissipative dynamical equation, e.g., quantum master equation. Under the Born approximation, full density operator can be factorized as $\hat{\rho}_{\text{tot}}(t)\approx\hat{\rho}_s(t)\otimes\hat{\rho}_{b,q}\otimes\hat{\rho}_{b,c}$,[72] where $\hat{\rho}_s(t)$ denotes the reduced system density operator, $\hat{\rho}_{b,\nu}=\exp(-\beta_\nu\hat{H}_{b,\nu})/Z_\nu$ describes the equilibrium distribution of the ν-th bosonic reservoir with the partition function $Z_\nu=\text{Tr}_b\{\exp(-\beta_\nu\hat{H}_{b,\nu})\}$, the inverse temperature $\beta_\nu=1/k_BT_\nu$, and the Boltzmann constant k_B set to be $k_B=1$. By separately perturbing $\hat{V}_q$ and $\hat{V}_c$, we obtain the dissipative dynamics of reduced system density operator by further including the Markov approximation.[56] This yields the quantum master equation

$$\frac{\text{d}}{\text{d}t}\hat{\rho}_s=\text{i}[\hat{\rho}_s,\hat{H}_s]+\sum_{n,\nu=q,c}\hat{\mathcal{L}}_{n\nu}[\hat{\rho}_s], \tag{6}$$

where the dissipator operator is specified as $\hat{\mathcal{L}}_{n,\nu}[\hat{\rho}_s]=[\hat{A}_{n,\nu},\hat{\rho}_s\tilde{\hat{A}}_{n,\nu}^\dagger]+\text{H.c.}$, with the modified operator $\tilde{\hat{A}}_{n,\nu}=\int_0^\infty\text{d}\tau C_{n,\nu}(\tau)\hat{A}_{n,\nu}(-\tau)$, the correlation function $C_{n,\nu}(\tau)=\sum_k|g_{n,k,\nu}|^2[N_{k,\nu}^B\,\text{e}^{\text{i}\omega_{\nu,k}\tau}+(1+N_{k,\nu}^B)\,\text{e}^{-\text{i}\omega_{\nu,k}\tau}]$, and the Bose–Einstein distribution function $N_{k,\nu}^B=1/[\exp(\omega_{k,\nu}/k_BT_\nu)-1]$. The coupling operators are specified as $\hat{A}_{n,q}=\hat{\sigma}_x^n$ and $\hat{A}_{n,c}=(\hat{a}_n^\dagger+\hat{a}_n)$.

We should admit that it is quite challenging to obtain the eigenspectrum of the anisotropic Rabi lattice model. While in the weak inter-site photon tunneling limit, one may approximately consider the mean-field approximation to reduce the anisotropic Rabi lattice to the effective single-site aQRM model, as carried out in various previous studies.[22–24,31] Technically, the inter-site photon tunneling terms can be effectively decoupled as $\hat{a}_n^\dagger\hat{a}_m\approx\langle\hat{a}_n^\dagger\rangle\hat{a}_m+\hat{a}_n^\dagger\langle\hat{a}_m\rangle-\langle\hat{a}_n^\dagger\rangle\langle\hat{a}_m\rangle$. Once the lattice sites are homogeneously arranged, which leads to the real order parameter of photons $\varphi=\langle\hat{a}_n^\dagger\rangle=\langle\hat{a}_m\rangle$. Such nonzero order parameter φ is generally used to characterize the delocalization of photons in the anisotropic Rabi lattice, i.e. the QPT of light.[33,34] Therefore, the mean-field expression of the reduced Hamiltonian of the anisotropic Rabi lattice is given by $\hat{H}_s'=\sum_n\hat{H}_{\text{MF}}^n(\varphi)$, where the single-site effective aQRM model in Fig. 1(b) is described as

$$\hat{H}_{\text{MF}}^n(\varphi)=\hat{H}_n^{\text{aRabi}}-zt\varphi(\hat{a}_n^\dagger+\hat{a}_n)+zt\varphi^2, \tag{7}$$

where z denotes the nearest-neighbor coordination number of the square resonators lattice, specified to be 4 in this study.[67]

By analyzing Eq. (7), it is known that the picture of inter-site photon tunneling now is changed to the effective external driving onto the on-site photons with the control parameter φ.[24,31]

Then, the modified operator is simplified as

$$\tilde{\hat{A}}_{n,\nu} \approx \int_0^\infty \mathrm{d}\tau C_{n,\nu}(\tau)\, \mathrm{e}^{-\mathrm{i}\tau \hat{H}^n_{\mathrm{MF}}(\varphi)} \hat{A}_{n,\nu}\, \mathrm{e}^{\mathrm{i}\tau \hat{H}^n_{\mathrm{MF}}(\varphi)}.$$

Under the mean-field framework, the effective lattice model on each site are identical. The system density operator maybe properly decomposed as $\hat{\rho}_{\mathrm{s}}(t) \approx \Pi_n[\hat{\rho}^n_{\mathrm{MF}}(t)]$. Finally, for each site the reduced master equation can be described as

$$\frac{\mathrm{d}}{\mathrm{d}t}\hat{\rho}^n_{\mathrm{MF}} = \mathrm{i}[\hat{H}^n_{\mathrm{MF}}(\varphi), \hat{\rho}^n_{\mathrm{MF}}] + \sum_{\nu=q,c} \{[\hat{A}_{n,\nu}, \hat{\rho}_{\mathrm{s}} \tilde{\hat{A}}^\dagger_{n,\nu}] + \mathrm{H.c.}\}. \quad (8)$$

We note that through the mean-field master equation simplifies the steady-state solution in the weak inter-site photon tunneling limit, it has its own limitations, e.g., it may miss the finite-size scaling, long-range correlation, and band structure of the aQRM lattice model.[31,34]

In the eigenbasis of $\hat{H}^n_{\mathrm{MF}}$, the off-diagonal elements of the reduced system density matrix at steady state generally show negligible contribution to steady-state behaviors, which is also numerically confirmed. Therefore, the master equation after long time evolution can be expressed as[55,56]

$$\begin{aligned}\frac{\mathrm{d}}{\mathrm{d}t}\hat{\rho}_{\mathrm{MF}} =\ & \mathrm{i}[\hat{\rho}_{\mathrm{MF}}, \hat{H}_{\mathrm{MF}}(\varphi)] \\ & + \sum_{l>j;\nu=q,c} \{\Gamma^-_\nu(\Delta_{lj})\hat{D}[|\psi_j\rangle\langle\psi_l|]\hat{\rho}_{\mathrm{MF}} \\ & + \Gamma^+_\nu(\Delta_{lj})\hat{D}[|\psi_l\rangle\langle\psi_j|]\hat{\rho}_{\mathrm{MF}}\}, \end{aligned} \quad (9)$$

where the dissipator is specified as $\hat{D}[\hat{O}]\hat{\rho}_{\mathrm{MF}} = (\hat{O}\hat{\rho}_{\mathrm{MF}}\hat{O}^\dagger - \hat{O}^\dagger\hat{O}\hat{\rho}_{\mathrm{MF}}/2 - \hat{\rho}_{\mathrm{MF}}\hat{O}^\dagger\hat{O}/2)$, and the subindex n is ignored with safety. The transition rates from incoherent dissipative exchange processes are given by $\Gamma^+_\nu(\Delta_{lj}) = \gamma_\nu(\Delta_{lj})N^{\mathrm{B}}_\nu(\Delta_{lj})|\langle\psi_l|\hat{A}_\nu|\psi_j\rangle|^2$ and $\Gamma^-_\nu(\Delta_{lj}) = \gamma_\nu(\Delta_{lj})[1 + N^{\mathrm{B}}_\nu(\Delta_{lj})]|\langle\psi_l|\hat{A}_\nu|\psi_j\rangle|^2$, where the spectral function of the ν-th reservoir is characterized as $\gamma_\nu(\Delta_{lj}) = 2\pi\sum_k |g_{k,\nu}|^2\delta(\omega_{k,\nu} - \Delta_{lj})$, the Bose–Einstein distribution function is $N^{\mathrm{B}}_\nu(\Delta_{lj}) = 1/[\exp(\Delta_{lj}/k_{\mathrm{B}}T_\nu) - 1]$, the energy gap becomes $\Delta_{lj} = E_l - E_j$ with the eigenvalues and corresponding eigenvectors $\hat{H}_{\mathrm{MF}}(\varphi)|\psi_j\rangle = E_j|\psi_j\rangle$, T_ν means the temperature in the ν-th reservoir, and k_{B} is the Boltzmann constant set to be 1. The operators are given by $\hat{A}_q = \hat{\sigma}_x$ and $\hat{A}_{\mathrm{c}} = (\hat{a}^\dagger + \hat{a})$. In this study we specify the spectral function as $\gamma_\nu(\omega) = \pi\alpha_\nu\omega\exp(-\omega/\omega_{\mathrm{c}})$, where α_ν is the dissipation strength and ω_{c} is the cut-off frequency of the reservoirs. ω_{c} is chosen sufficiently large to validate the Born approximation, e.g., $\omega_{\mathrm{c}} = 20\omega_0$.

We focus on steady-state behavior of the dissipative anisotropic Rabi lattice, which can be iteratively obtained based on the dressed master equation at Eq. (9). Starting from one test φ_{in}, we solve Eq. (9) to obtain the corresponding density operator $\hat{\rho}_{\mathrm{out}}$. We can get a updated parameter $\varphi_{\mathrm{out}} = \mathrm{Tr}\{\hat{\rho}_{\mathrm{out}}\hat{a}\}$. Then we check whether the relative error $\mathrm{err} = |(\varphi_{\mathrm{out}} - \varphi_{\mathrm{in}})/\varphi_{\mathrm{in}}|$ is below the set tolerance (set to be 10^{-4} in this study). If not, we continue a new round iteration with the assignment $\varphi_{\mathrm{in}} = \varphi_{\mathrm{out}}$. If fulfilled, then we define φ_{out} as the approximate order parameter of photons, and $\hat{\rho}_{\mathrm{out}}$ becomes the steady state $\hat{\rho}_{\mathrm{ss}}$. In this work, we set the maximum truncation number of photons as $N_{\mathrm{tr}} = 50$, which is sufficient to confirm the convergence of steady-state results. We show steady-state order parameter of photons $|\varphi|$ by modulating the qubit–photon coupling strength λ and anisotropic factor γ in Fig. 1(c). It is generally found that the order parameter is monotonically enhanced by increasing the inter-site photon tunneling strength t and anisotropic factor γ.

3. Two-photon correlation function

3.1. Definition in the dressed picture

Two-photon correlation function was considered as one main feature to characterize the nonclassicality of photons in quantum optics. It was initially proposed by Glauber to study the quantum coherence of radiation field,[73] which is quantified as

$$G^{(2)}(\tau, t) = \frac{\langle \hat{a}^\dagger(t)\hat{a}^\dagger(t+\tau)\hat{a}(t+\tau)\hat{a}(t)\rangle}{\langle \hat{a}^\dagger(t)\hat{a}(t)\rangle^2}, \quad (10)$$

where $\langle\hat{O}(t)\rangle = \mathrm{Tr}\{\hat{O}\hat{\rho}_{\mathrm{s}}(t)\}$ denotes the expected value with t-time reduced system density operator. It is already known that at weak qubit–photon coupling the output detection field operator is proportional to the cavity–photon operator. Hence, the two-photon statistics of output field can be described by Eq. (10). In particular, bunching and anti-bunching of photons are two typical nontrivial behaviors of quantum light. Specifically, $G^{(2)}(\tau, t) > 1$ denotes the photon bunching effect, $G^{(2)}(\tau, t) < 1$ means the antibunching effect, and $G^{(2)}(\tau, t) = 1$ corresponds to the photon coherent state. Moreover, $G^{(2)}(\tau, t) = 2$ occurs at thermal equilibrium distribution of photons.

While as the qubit–photon coupling becomes strong, this definition of two-photon correlation function should be redefined in the dressed picture of the quantum systems. Alternatively, Ridolfo *et al.* modified the input–output relation based on the dressed states,[46,48] with the detection field operator expressed as

$$\hat{X}^- = -\mathrm{i}\sum_{E_k > E_j} \Delta_{k,j} X_{k,j} |\psi_j\rangle\langle\psi_k|, \quad (11)$$

with the energy gap $\Delta_{k,j} = E_k - E_j$, the detection coefficient $X_{k,j} = \langle\psi_j|(\hat{a}^\dagger + \hat{a})|\psi_k\rangle$. Consequently, two-photon correla-

tion function can be reexpressed as

$$G^{(2)}(\tau,t)=\frac{\langle\hat{X}^{+}(t)\hat{X}^{+}(t+\tau)\hat{X}^{-}(t+\tau)\hat{X}^{-}(t)\rangle}{\langle\hat{X}^{+}(t)\hat{X}^{-}(t)\rangle^{2}}. \tag{12}$$

At steady state, two-photon correlation function is given by

$$G^{(2)}(\tau)=\frac{\langle\hat{X}^{+}\hat{X}^{+}(\tau)\hat{X}^{-}(\tau)\hat{X}^{-}\rangle_{\rm ss}}{\langle\hat{X}^{+}\hat{X}^{-}\rangle_{\rm ss}^{2}}. \tag{13}$$

3.2. Effective anisotropic Rabi case

We first investigate the effects of qubit–photon coupling and anisotropic factor on zero-time-delay two-photon correlation function in the effective aQRM at steady state in Fig. 2. In absence of inter-site photon tunneling (i.e. $t=0$) in Fig. 2(a), the effective aQRM is naturally reduced to the aQRM ($\varphi=0$). It is intriguing to find that with finite anisotropic factor, e.g., $\gamma=0.5$, there exists second novel anti-bunching to bunching transition of photons by increasing qubit–photon coupling strength, except the traditional nonclassical transition in the standard QRM.[57] Hence, the anisotropic qubit–photon interactions dramatically extend the regime of nonclassical feature of photons. Then we tune on inter-site photon tunneling strength, e.g., $t=0.05\omega_0$ in Fig. 2(b). The novel anti-bunching behavior is significantly suppressed, whereas the bunching feature becomes significant, which can be also clearly exhibited in Fig. 2(d). If we further increase photon tunneling strength, the second anti-bunching to bunching transition is completely suppressed as shown in Fig. 2(c).

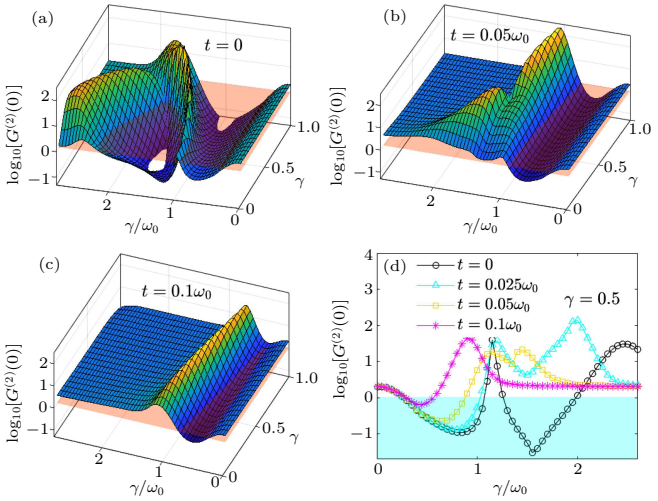


Fig. 2. Influences of the qubit–photon coupling strength λ and anisotropic factor γ on two-photon correlation function with distinct inter-site photon tunneling strengths (a) $t=0$, (b) $t=0.05\omega_0$, and (c) $t=0.1\omega_0$. (d) The behavior of two-photon correlation function by tuning λ with $\gamma=0.5$. Other system parameters are the same as those in Fig. 1.

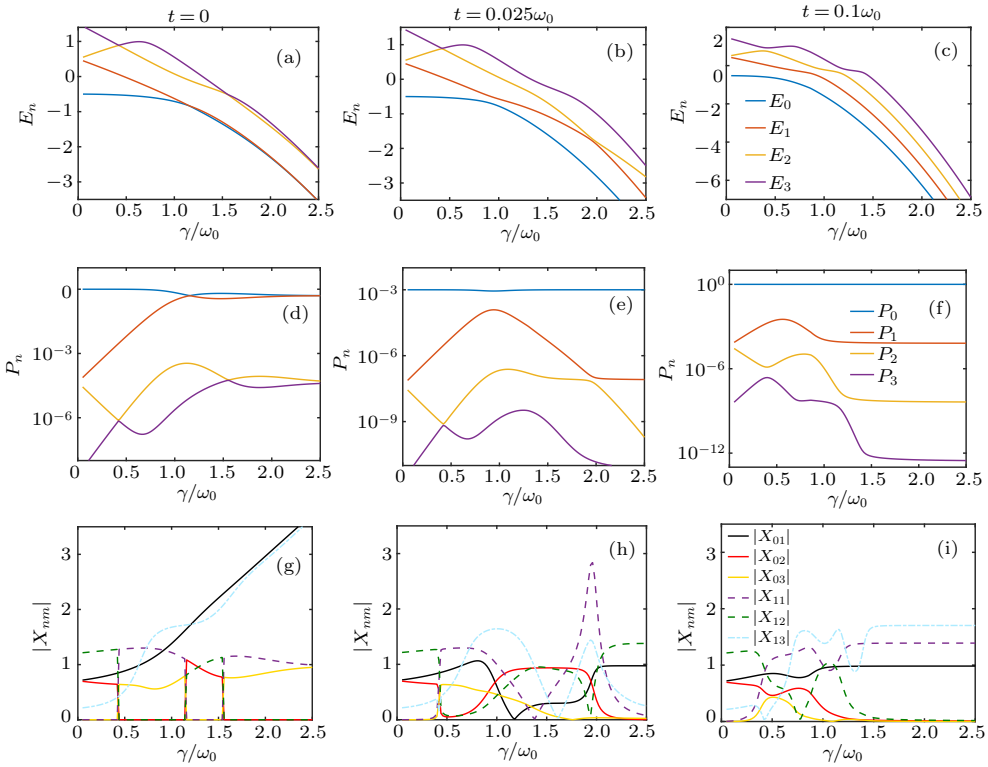


Fig. 3. (a)–(c) Four lowest eigenvalues, (d)–(f) steady-state populations, and (g)–(i) the transition coefficient X_{nm} in Eq. (12) as a function of qubit–photon coupling strength with distinct inter-site photon tunneling strengths and the anisotropic factor $\gamma=0.5$ in the effective aQRM. Other system parameters are identical with those in Fig. 1.

Then we try to explore the underlying mechanism of the influence of inter-site photon tunneling on the novel anti-bunching to bunching transition in the effective aQRM in Fig. 3. In the low temperature regime with weak excitation of the effective aQRM, based on Eq. (11) the effective photon occupation is given by $\langle\hat{X}^{+}\hat{X}^{-}\rangle_{\rm ss}\approx(\Delta_{10}X_{10})^2P_1$ with $P_n=\langle\psi_n|\hat{\rho}_{\rm MF}(\infty)|\psi_n\rangle$ the steady state population, and the two-photon correlation term is $\langle\hat{X}^{+}\hat{X}^{+}\hat{X}^{-}\hat{X}^{-}\rangle_{\rm ss}\approx P_2\mathcal{A}_2+$

$P_3\mathcal{A}_3$, with the transition coefficients given by $\mathcal{A}_n = \sum_{l<k<n}(\Delta_{n,k}\Delta_{k,l}X_{n,k}X_{k,l})^2$. The steady-state zero-time-delay two-photon correlation function in Eq. (13) can be approximately expressed as

$$G^{(2)}(0)\approx\frac{P_2\mathcal{A}_2+P_3\mathcal{A}_3}{(\Delta_{10}X_{10})^4P_1^2}. \tag{14}$$

For the traditional antibunching-to-bunching transition of photons in effective aQRM (e.g. $\gamma=0.5$ in Fig. 3), the microscopic processes in effective aQRM are similar to the standard QRM.[57] When increasing the qubit–photon, e.g., $\lambda\approx0.8\omega_0$ with $t=0,0.025\omega_0$ and $\lambda\approx0.5\omega_0$ with $t=0.1\omega_0$, the first energy gap Δ_{10} quickly decreases compared to Δ_{21}, as shown in Figs. 3(a)–3(c). Thus the first excited state population shows dramatic enhancement in Figs. 3(d)–3(f). Moreover, by analyzing transition coefficients in Figs. 3(g)–3(i), it is found that the two-photon correlation term is dominant by the transition process $|\psi_0\rangle\to|\psi_1\rangle\to|\psi_2\rangle$. Then the two-photon correlation function at Eq. (14) is simplified as

$$G^{(2)}(0)\approx\frac{(\Delta_{2,1}\Delta_{1,0}X_{2,1}X_{1,0})^2P_2}{(\Delta_{10}X_{10})^4P_1^2}\propto\frac{P_2}{P_1^2}. \tag{15}$$

The dramatic increase of P_1 compared to P_2 in Fig. 3(d) yields the photon blockade. While for the traditional photon bunching, e.g., $\lambda\approx1.2\omega_0$ with $t=0,0.025\omega_0$, two-photon correlation function is reduced to

$$G^{(2)}(0)\approx\frac{\mathcal{A}_3P_3}{(\Delta_{10}X_{10})^4P_1^2}\propto\frac{P_3}{P_1^2}. \tag{16}$$

The comparative increase of Δ_{10} significantly suppresses P_1, as shown in Figs. 3(d) and 3(e), which consequently lifts up $G^{(2)}(0)$.

Next we analyze the second antibunching feature in aQRM with $t=0$, e.g., $\lambda\approx1.6\omega_0$ in Fig. 2(d). It is found that two-photon correlation function is approximately expressed as Eq. (15). The decrease of gap Δ_{10} in Fig. 3(a) enhances first-excited state population P_1 in Fig. 3(d), which leads to this novel photon blockade. Once we slightly tune on inter-site photon tunneling, e.g., $t=0.025\omega_0$, the expression of two-photon correlation function is identical with Eq. (15). However, the eigenspectrum is quite distinct from the one with $t=0$. Specifically, with qubit–photon coupling strength around $1.6\omega_0$, Δ_{10} shows is dramatically enlarged, which suppresses P_1. Thus $G^{(2)}(0)$ is enhanced, i.e., antibunching becomes vanishing. While by further increasing qubit–photon coupling, e.g., $\lambda\lesssim2\omega_0$, it is interesting to find that the gap Δ_{21} shrinks monotonically, leading to the persistent decrease of P_1, which exhibits the second giant bunching effect of photons. If we increase inter-site photon tunneling strength to $t=0.1\omega_0$, there is no signature of additional photon antibunching at strong qubit–photon coupling, e.g., $\lambda\gtrsim1.5\omega_0$. The main reason is that the eigenvalues are almost uniformly spaced in Fig. 3(c), due to the dramatic influence of mean-field driving term $zt\varphi(\hat{a}^\dagger+\hat{a})$ in Eq. (7) on formation of the coherent eigenstates. Therefore, the inclusion of inter-site photon tunneling is detrimental to photon antibunching with strong qubit–photon coupling, in particular at strong tunneling regime. While it becomes helpful to exhibit photon bunching with slight tunneling strength.

We also study the influence of multiple qubits on two-photo correlation function in Fig. 4 with the system Hamiltonian described in Eq. (5). By increasing the number of qubits, it is generally found that both antibunching and bunching behaviors of photons are gradually suppressed. While for fixed inter-site photon tunneling, the nonclassical feature of photons can be amplified by increasing anisotropic factor γ, e.g., comparing Fig. 4(a) [4(b)] with Fig. 4(c) [4(d)].

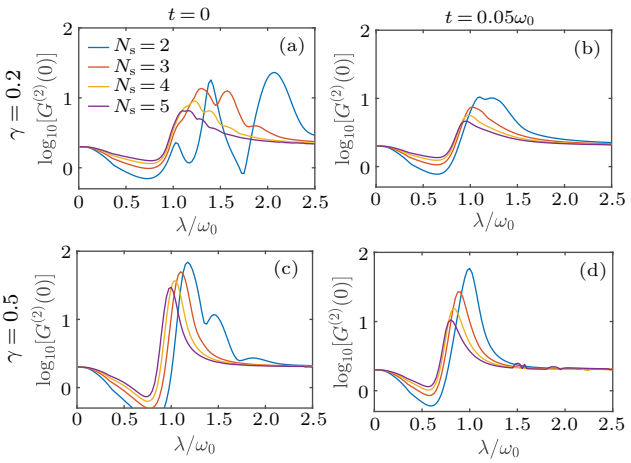


Fig. 4. Two-photon correlation function with finite qubits numbers as a function of λ with distinct t and γ. Other system parameters are identical with those in Fig. 1.

4. Quadrature squeezing

Photon squeezing is also regarded as one main characteristic to capture nonclassicality of photons.[74] Light is considered to be a squeezed state once the amplitude or phase has a reduced quantum uncertainty compared with the counterpart of coherent state.[53] While here quadrature squeezing means the fluctuation of one quadrature component breaks the Heisenberg noise limit at vacuum, whereas the other component surpasses such vacuum limit due to the Heisenberg uncertainty relation.[51,52,75] The steady-state quadrature squeezing factor to quantify the photon squeezing is characterized as[76]

$$\xi^2_{\rm QS}=\min_{\theta\in[0,2\pi)}\langle(\Delta\hat{X}_\theta)^2\rangle_{\rm ss}, \tag{17}$$

where the generalized canonical coordinate variable denotes $\hat{X}_\theta=\hat{X}\cos\theta+\hat{P}\sin\theta$, the reduced position and momentum operators become $\hat{X}=(\hat{a}^\dagger+\hat{a})$ and $\hat{P}=\mathrm{i}(\hat{a}^\dagger-\hat{a})$, respectively, and θ is the detection angle to search the minimal squeezing factor $\xi^2_{\rm QS}$. In literature, the photon squeezing emerges once $\xi^2_{\rm QS}<1$, whereas $\xi^2_{\rm QS}>1$ denotes the disappearance of the photons squeezing. And $\xi^2_{\rm QS}=1$ corresponds to the coherent state mode of photons.

We first study the effects of qubit–photon coupling λ and anisotropic factor γ on the quadrature squeezing in Fig. 5. By increasing the anisotropic factor it is found that the photon squeezing persists both with and without inter-site photon tunnelings in Figs. 5(a) and 5(b), respectively. Such feature becomes more clear in Fig. 5(c) as we exhibit the global minimal of $\xi^2_{\rm QS}$ by modulating qubit–photon coupling strength, i.e., $\min_\lambda\{\xi^2_{\rm QS}\}$. Moreover, the inclusion of inter-site photon tunneling is helpful to enhance quadrature squeezing at small anisotropic factor regime, e.g., $\gamma = 0.1$. We also investigate the influence of temperature on $\min_\lambda\{\xi^2_{\rm QS}\}$ in Fig. 5(d). Generally, the reservoirs' temperatures are detrimental to establish quadrature squeezing. Next we study the $\xi^2_{\rm QS}$ in the effective Dicke model with finite qubits numbers in Fig. 6. Intriguingly, the quadrature squeezing is dramatically enhanced by increasing the number of qubits at strong qubit–photon coupling, e.g., $1\lesssim\lambda/\omega_0\lesssim 3$. Therefore, quadrature squeezing benefits from multiple qubits both in effective anisotropic and standard Dicke models.

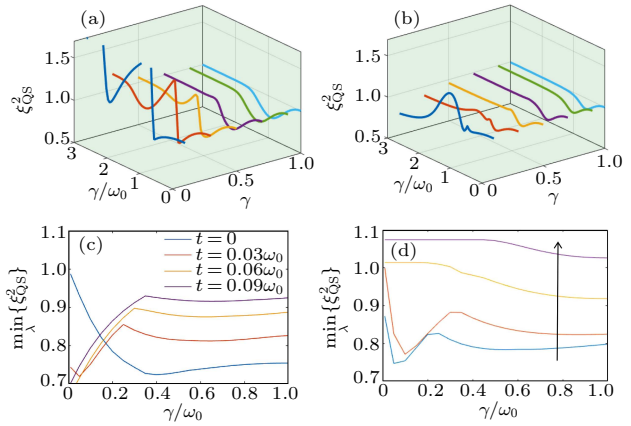


Fig. 5. Quadratic squeezing factor $\xi^2_{\rm QS}$ (a) $t = 0$ and (b) $t = 0.05\omega_0$ as functions of qubit–photon coupling and anisotropic factor at $k_{\rm B}T_{\rm c} = k_{\rm B}T_q = 0.01\omega_0$. The minimization of $\xi^2_{\rm QS}$ by tuning λ (c) with distinct t at $k_{\rm B}T_{\rm c} = k_{\rm B}T_q = 0.01\omega_0$ and (d) with $t = 0.02$ and $k_{\rm B}T_{\rm c}/\omega_0 = k_{\rm B}T_q/\omega_0 = 0.01, 0.1, 0.2, 0.3$ from bottom to up. Other system parameters are identical with those in Fig. 1.

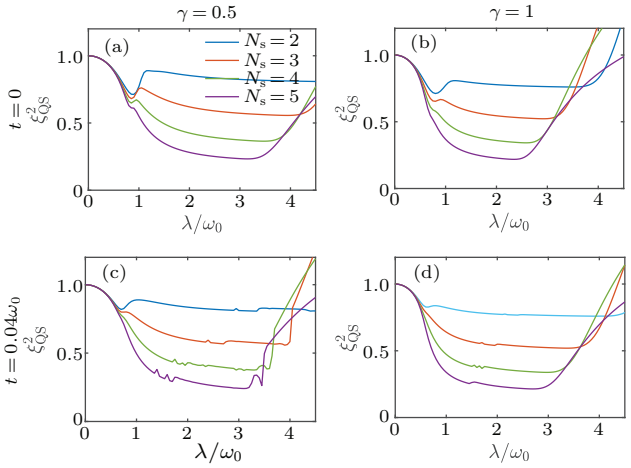


Fig. 6. Quadratic squeezing factor $\xi^2_{\rm QS}$ as a function of λ with the finite qubits number. Other system parameters are given by $\omega_0 = 1$, $\varepsilon = \omega_0$, $z = 4$, $\alpha_q = \alpha_{\rm c} = 10^{-4}$, $\omega_{\rm c} = 20\omega_0$, and $k_{\rm B}T_{\rm c} = k_{\rm B}T_q = 0.01\omega_0$.

5. Conclusion

To summarize, we studied nonclassical behaviors of photons in an open anisotropic Rabi lattice model. The quantum dressed master equation embedded with mean-field approximation is included to consider quantum dissipation stemming from the interactions between quantum system components and bosonic thermal reservoirs. We first investigated influences of strong qubit–photon coupling and anisotropic factor on two-photon correlation function. In absence of inter-site photon tunneling, the novel photon antibunching is unravelled, which is absent in standard QRM. By including inter-site photon tunneling, such photon antibunching feature is dramatically suppressed, whereas the photon bunching is robust at weak inter-site photon tunneling. Moreover, the finite number of qubits is detrimental to the formation of photon blockade.

We also analyzed quadrature squeezing in the effective anisotropic quantum Rabi model. The photon squeezing persists both with and without inter-site photon tunnelings. The inclusion of inter-site photon tunneling is helpful for enhancing quadrature squeezing with the small anisotropic factor. And quadrature squeezing is significantly strengthened by increasing qubits number at strong qubit–photon coupling. Moreover, we studied the effect of temperatures of thermal reservoirs on global minimization of quadrature squeezing factor by tuning qubit–photon coupling, which demonstrates that finite temperature is detrimental to the formation of photon squeezing. We note that this work is carried out under the mean-field approximation in the weak inter-site photon tunneling limit,[23] where quantum fluctuation induced by the inter-photon tunneling is comparatively negligible to the on-site qubit–photon coupling. And it should be intriguing to explore the nonclassical features of photons with strong inter-site photon tunneling.[34]

In quantum optics, generation of single-photon source, e.g., photon antibunching effect, and photon squeezing in photonic lattices is regarded as one significant research direction.[42,43,77,78] We hope that the obtained nonclassical features of photons by modulating inter-site photon tunneling and anisotropic qubit–photon coupling may deepen the understanding and fertilize the operation of photons in photonic nanostructures.

Acknowledgements

Project supported by the National Natural Science Foundation of China (Grant No. 11874011) and the Opening Project of Shanghai Key Laboratory of Special Artificial Microstructure Materials and Technology.

References

[1] Tannoudji C C, Roc J D and Grynberg G 1998 *Atom-photon interactions: basic processes and applications* (New York: John Wiley and Sons)

[2] Haroche S, Brune M and Raimond J M 2020 *Nat. Phys.* **16** 243
[3] Blais A, Girvin S M and Oliver W D 2020 *Nat. Phys.* **16** 247
[4] Scully M O, Zubairy M S, Agarwal G S and Walther H 2003 *Science* **299** 862
[5] Ronzani A, Karimi B, Senior J, Chang Y C, Peltonen J T, Chen C D and Pekola J P 2018 *Nat. Phys.* **14** 991
[6] Raimond J M, Brune M and Haroche S 2001 *Rev. Mod. Phys.* **73** 565
[7] Blais A, Grimsmo A L, Girvin S M and Wallraff A 2021 *Rev. Mod. Phys.* **93** 025005
[8] Niemczyk T, Deppe F, Huebl H, Menzel E P, Hocke F, Schwarz M J, Garcia-Ripoll J J, Zueco D, Hummer T, Solano E, Marx A and Gross R 2010 *Nat. Phys.* **6** 772
[9] Yoshihara F, Fuse T, Ashhab S, Kakuyanagi K, Saito S and Semba K 2017 *Nat. Phys.* **13** 44
[10] Kockum A F, Miranowicz A, Liberato S De, Savasta S and Nori F 2019 *Nat. Rev. Phys.* **1** 19
[11] Forn-Díaz P, Lamata L, Rico E, Kono J and Solano E 2019 *Rev. Mod. Phys.* **91** 025005
[12] Xie Q T, Cui S, Cao J P, Amico J and Fan H 2014 *Phys. Rev. X* **4** 021046
[13] Tomka M, Araby O E, Pletyukhov M and Gritsev V 2014 *Phys. Rev. A* **90** 063839
[14] Zhang Y Y and Chen X Y 2017 *Phys. Rev. A* **96** 063821
[15] Forn-Díaz P, Lisenfeld J, Marcos D, García-Ripoll J J, Solano E, Harmans C J P M and Mooij J E 2010 *Phys. Rev. Lett.* **105** 237001
[16] Rashba E I 1960 *Sov. Phys. Solid State* **2** 1109
[17] Dresselhaus G 1955 *Phys. Rev.* **100** 580
[18] Hwang M J, Kim M S and Choi M S 2016 *Phys. Rev. Lett.* **116** 153601
[19] Mao B B, Li L S, You W L and Liu M X 2021 *Physica A* **564** 125534
[20] Ma K K W 2020 *Phys. Rev. A* **102** 053709
[21] Zhang Y Y, Hu Z X, Fu L B, Luo H G, Pu H and Zhang X F 2021 *Phys. Rev. Lett.* **127** 063602
[22] Hartmann M, Brandao F and Plenio M 2006 *Nat. Phys.* **2** 849
[23] Greentree A D, Tahan C, Cole J H and Hollenberg L C 2006 *Nat. Phys.* **2** 856
[24] Koch J and Hur K L 2009 *Phys. Rev. A* **80** 023811
[25] Hwang M J and Plenio M 2016 *Phys. Rev. Lett.* **117** 123602
[26] Chen Z H, Wang F Y, Chen H, Lu J C and Wang C 2023 *Chin. Phys. Lett.* **40** 050501
[27] Cirac J I, Zoller P, Kimble H J and Mabuchi H 1997 *Phys. Rev. Lett.* **78** 3221
[28] Kimble H J 2008 *Nature* **453** 1023
[29] Zhou L, Yang L P, Li Y and Sun C P 2013 *Phys. Rev. Lett.* **111** 103604
[30] Peng J, Zheng J C, Yu J, Tang P H, Barrios G A, Zhong J X, Solano E, Arriagada F A and Lamata L 2021 *Phys. Rev. Lett.* **127** 043604
[31] Hur K L, Henriet L, Petrescu A, Plekhanov K, Roux G and Schiro M 2016 *C. R. Phys.* **17** 808
[32] Carusotto I and Ciuti C 2013 *Rev. Mod. Phys.* **85** 299
[33] Zheng H and Takada Y 2011 *Phys. Rev. A* **84** 043819
[34] Schiro M, Bordyuh M, Oztop B and Tureci H E 2012 *Phys. Rev. Lett.* **109** 053601
[35] Lu Y C and Wang C 2016 *Quantum Inf. Process.* **15** 4347
[36] Ma J L, Liu B B, Li Q, Guo Z X, Tan L and Ying L 2024 *Phys. Rev. A* **109** 033703
[37] Azzam S I, Shalaev V M, Boltasseva A and Kildishev A V 2018 *Phys. Rev. Lett.* **121** 253901
[38] Aigner A, Tittl A, Wang J, Weber T, Kivshar Y, Maier S A and Ren H R 2022 *Sci. Adv.* **8** eadd4816
[39] Hu Z C, Bongiovanni D, Jukic D, Jajtic E, Xia S Q, Song D H, Xu J J, Morandotti R, Buljan H and Chen Z G 2021 *Light: Sci. Appl.* **10** 164
[40] Jurgensen M, Mukherjee S and Rechtsman M C 2021 *Nature* **596** 63
[41] Wang P, Fu Q D, Peng R H, Kartashov Y V, Torner L, Konotop V V and Ye F W 2022 *Nat. Commun.* **13** 6738
[42] Roy D, Wilson C M and Firstenberg O 2017 *Rev. Mod. Phys.* **89** 021001
[43] Chang D E, Douglas J, Gonzalez-Tudela A, Hung C L and Kimble H J 2018 *Rev. Mod. Phys.* **90** 031002
[44] Uppu R, Pedersen F T, Wang Y, Olesen C T, Papon C, Zhou X Y, Midolo L, Scholz S, Wieck A D, Ludwig A and Lodahl P 2020 *Sci. Adv.* **6** eabc8268
[45] Zhang J F, Chattaraj S, Huang Q, Jordao L, Lu S Y and Madhukar A 2022 *Sci. Adv.* **8** eabn9252
[46] Rabl P 2011 *Phys. Rev. Lett.* **107** 063601
[47] Ding Z and Zhang Y 2022 *Chin. Phys. B* **31** 070304
[48] Ridolfo A, Leib M, Savasta S and Hartmann M 2012 *Phys. Rev. Lett.* **109** 193602
[49] Carmichael H J 1999 *Statistical Methods in Quantum Optics 1, Master Equations and Fokker Planck Equations* (Springer)
[50] Zhang X Y, Wang J S, Wang L, Meng X G and Liang B L 2022 *Chin. Phys. B* **31** 054205
[51] Stoler D 1970 *Phys. Rev. D* **1** 3217
[52] Stoler D 1971 *Phys. Rev. D* **4** 1925
[53] Ficek Z and Drummond P D 1997 *Phys. Today* **50** 34
[54] Glauber R J 1963 *Phys. Rev.* **130** 2529
[55] Beaudoin F, Gambetta J M and Blais A 2011 *Phys. Rev. A* **84** 043832
[56] Settineri A, Macri V, Ridolfo A, Stefano O Di, Kockum A F, Nori F and Savasta S 2018 *Phys. Rev. A* **98** 053834
[57] Ridolfo A, Savasta S and Hartmann M 2013 *Phys. Rev. Lett.* **110** 163601
[58] Loudon R and Knight P 1987 *J. Mod. Opt.* **34** 709
[59] Kolobov M I 1999 *Rev. Mod. Phys.* **71** 1539
[60] Gerry C and Knight P 2004 *Introductory Quantum Optics* (London: Cambridge University Press)
[61] Kronwald A, Marquardt F and Clerk A A 2013 *Phys. Rev. A* **88** 063833
[62] Wollman E E, Lei C U, Weinstein A J, Suh J, Kronwald A, Marquardt F, Clerk A A and Schwab K C 2015 *Science* **349** 952
[63] Liao J Q and Law C K 2011 *Phys. Rev. A* **83** 033820
[64] Lv X Y, Liao J Q, Tian L and Nori F 2015 *Phys. Rev. A* **91** 013834
[65] Xie J K, Ma S L, Ren Y L, Li X K and Li F L 2020 *Phys. Rev. A* **101** 012348
[66] Wang C, Chen H and Liao J Q 2021 *Phys. Rev. A* **104** 033701
[67] Hohenadler M, Aichhorn M, Pollet L and Schmidt S 2012 *Phys. Rev. A* **85** 013810
[68] Dimer F, Estienne B, Parkins A S and Carmichael H J 2007 *Phys. Rev. A* **75** 013804
[69] Buijsman W, Gritsev V and Sprik R 2017 *Phys. Rev. Lett.* **118** 080601
[70] Houck A A, Tureci H E and Koch J 2012 *Nat. Phys.* **8** 292
[71] Raftery J, Sadri D, Schmidt S, Tureci H E and Houck A A 2014 *Phys. Rev. X* **4** 031043
[72] Weiss U 2012 *Quantum Dissipative Dynamics* (Singapore: World Scientific)
[73] Glauber R J 1963 *Phys. Rev.* **130** 2529
[74] Walls D F 1983 *Nature* **306** 5939
[75] Andersen U L, Gehring T, Marquardt C and Leuchs G 2016 *Phys. Scr.* **91** 053001
[76] Ma J, Wang X G, Sun C P and Nori F 2011 *Phys. Rep.* **509** 89
[77] Ren R J, Lu Y H, Jiang Z K, Gao J, Zhou W H, Wang Y, Jiao Z Q, Wang X W, Solntsev A S and Jin X M 2022 *Photon. Res.* **10** 456
[78] Zhu H H, Chen H S, Chen T, Li Y, Luo S B, Karim M F, Luo X S, Gao F, Li Q, Cai H, Chin L K, Kwek L C, Norden B, Zhang X D and Liu A Q 2024 *Nat. Commun.* **15** 6057